RSC Advances

Dynamic Article Links

Cite this: *RSC Advances*, 2012, **2**, 1639–1642

www.rsc.org/advances

PAPER

Two dimensional thermoelectric platforms for thermocapillary droplet actuation

Man-Chi Liu,[ac] Jin-Gen Wu,[a] Ming-Fei Tsai,[a] Wei-Shun Yu,[a] Pei-Chun Lin,*[a] I-Chung Chiu,[b] Huai-An Chin,[b] I-Chun Cheng,[b] Yi-Chung Tung[c] and Jian-Zhang Chen*[d]

Received 14th October 2011, Accepted 8th November 2011
DOI: 10.1039/c1ra00896j

Thermocapillary droplet actuation on a substrate is based on the mechanism that droplets can be driven to the cooler regions *via* surface tension modulation by varying the temperature. The usual method of providing a temperature gradient or temperature difference for thermocapillary droplet actuation is *via* resistor heaters, in which the rise in temperature can be achieved by increasing the passing currents, yet the cooling function relies on the natural conduction and/or convection. A thermoelectric (TE) chip is advantageous in the temperature control. The heating and cooling functions can be manipulated simply by adjusting the direction of the input current into the TE chip. In this regard, the temperature setting can be precisely feedback-controlled by manipulating the amplitude and direction of current flows. This paper demonstrates the implementation of a two dimensional (2D) TE array for free-surface thermocapillary droplet actuation. The routing, merging, and cutting of droplets are successfully demonstrated on a hydrophobically patterned glass substrate overlaid on the TE array.

1. Introduction

Thermocapillary liquid actuation has been extensively studied with droplets or bubbles placed in closed channels[1–9] or on open-surface substrates.[10–20] The investigation of fundamentals of free surface thermocapillary droplet actuation is still continued due to the complications concerning the interaction of drop molecules with the surface,[10,13,16–18] and the complexity of evaporation (at the receding contact line, hot side) and condensation (at the advancing contact line, cold side) when volatile liquid droplets are driven on open-surface substrates.[13,16,17] For a low vapor pressure liquid such as polydimethylsiloxane, it is experimentally difficult to conduct a true droplet migration experiment on partially wetting or completely wetting surfaces, because a tail is left behind after the droplet advances. It behaves more like shear thinning rather than droplet migration by a thermocapillary stress. The complications and uncertainty in experimental conditions make it difficult to precisely compare the experimental results with theoretical models.[13,16–18] Despite water droplets having been mobilized on well-cleaned SiO_2 surfaces,[13,21] in most cases, relatively polar liquid droplets, such as water or alcohol droplets, are difficult to mobilize on partially wettable surfaces,[16] possibly due to the lack of precursor films which ease the stress concentration at contact lines. Most recently, Zhao *et al.* demonstrated a water–heptanol binary drop thermocapillary actuation on a parylene-coated silicon substrate.[22] In their case, the heptanol liquid forms a precursor film to facilitate the advance of the droplet on a parylene coated surface.

In regard to the technical development, the temperature gradients are usually generated by resistance heaters,[1,2,7,13–18] while some optical heating schemes also have been developed.[8,20,23] The optical operation offers non-contact features, which can reduce the contamination *via* interface contacts. The advantages of the resistance heaters are low-cost, convenient to actuate, and easy to integrate onto the chips. Nevertheless, the precise temperature control could be problematic because the heating can be carried out simply by increasing the input current, yet the cooling can only rely on passive natural convection or conduction.

Motivated by the desire for flexibility and controllability in two-dimensional (2D) free-surface thermocapillary droplet manipulation, in this study, we report a novel approach utilizing a 5 × 5 array of thermoelectric (TE) chips. The advantage of using TE chips is their practical controllability in the bi-directional heat conduction. The heating and cooling functions can be simply manipulated by adjusting the direction and magnitude of current flowing through the TE chips. Together with the adequate heating and cooling of the TE chips beneath and around the actuated droplets, the droplets can be successfully routed, merged, and split according to the pre-planned

[a]*Department of Mechanical Engineering, National Taiwan University, Taipei 10617, Taiwan. E-mail: peichunlin@ntu.edu.tw; Fax: +886 2 2363 1755; Tel: +886 2 3366 9747*
[b]*Graduate Institute of Photonics and Optoelectronics & Department of Electrical Engineering, National Taiwan University, Taipei 10617, Taiwan*
[c]*Research Center for Applied Sciences, Academia Sinica, Taipei 11529, Taiwan*
[d]*Institute of Applied Mechanics, National Taiwan University, Taipei 10617, Taiwan. E-mail: jchen@ntu.edu.tw; Fax: +886 2 3366 5694; Tel: +886 2 3366 5694*

motion pattern realized by the pre-programmed thermal map sequence.

2. Experimental

Control system

The overall system is sketched in Fig. 1. Twenty-five TE chips with size 6 mm × 6 mm × 3.4 mm (TES1-007.21, Tande Energy and Temperature Associates pty. Co.) are arranged into a 5 × 5 2D array. For each of the 25 TE chips, one side of the TE chip surface (*i.e.*, the top surface) is used for droplet temperature modulations; the other side (*i.e.*, the bottom surface) is rigidly mounted onto an aluminium heat sink with a cooling fan, which regulates the temperature of the bottom surfaces of the TE chips. Each TE chip has three statuses: (i) heating, at which the temperature of the top surface ("sample" side) is higher than that of the bottom surface; (ii) cooling, *vice versa*; or (iii) idle, at which the TE chip is not actuated. The status of the TE chip is adjusted by two digital control channels, one for actuation (*i.e.*, either heating/cooling or idle) and the other for the determination of the activating status (*i.e.*, either heating or cooling). A 400 MHz real-time embedded system is utilized as the main computer (SbRIO-9602, National Instruments), which has onboard digital output (DO) channels ready for interfacing the TE chips. Because the embedded system SbRIO-9602 and the TE chip driving electronics are operated in different voltage and current ratings, the commercial relays (NA5W-K, Takamisawa) are utilized for the signal separation in this empirical implementation. The cooling fan is also controlled by a similar infrastructure to regulate the temperature of the aluminium heat sink (*i.e.*, also the bottom surfaces of the TE chips). The temperature of the heat sink is measured by a thermocouple, whose signal is sent to the embedded system SbRIO-9602 *via* the thermocouple input module (NI-9213, National Instruments). LabView 2009 (National Instruments) is adopted as the software infrastructure, and the control commands for the TE chips can be pre-programmed into the embedded system SbRIO-9602 or remotely controlled by the operator *via* a standard Ethernet or wireless protocol.

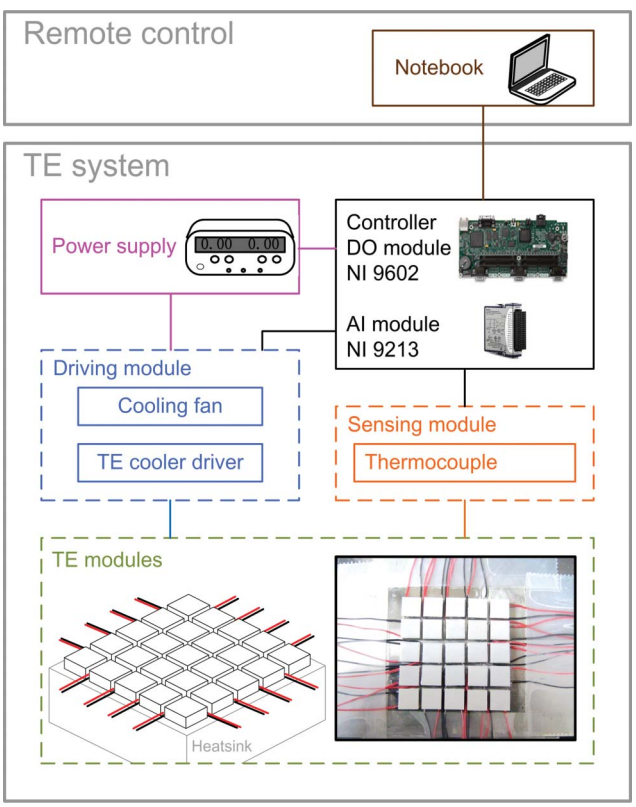

Fig. 1 Illustration of the platforms for the 2D TE array and the control system.

Sample fabrication

The wetting channels (stripes) are defined by a patterned self-assembled monolayer of 1*H*,1*H*,2*H*,2*H*-perfluorooctyl-trichlorosilane (PFOTS, Alfa Aesar) on 0.7 mm thick 5 cm × 5 cm glass substrates (Eagle-2000). The glass substrate is immersed in a 1 mM solution of PFOTS in dodecane (96%, TEDIA) at room temperature. The checkerboard wetting stripes (0.5 cm in width) are patterned by photolithography and covered with photoresist when conducting the monolayer deposition. Using the lift-off technique, the wetting regions can be clearly defined. The chemically patterned glass substrates were rinsed with acetone and isopropanol two times and blown dry.

3. Results and discussion

Fig. 2 shows the thermal cycle characteristic for a single TE chip. The temperature of the top surface can be cyclically switched between 5 °C and 78 °C. It demonstrates a reliable switching control over this temperature range. As described in Section 2, the TE chips are tightly packed into a 5 × 5 2D array to form a droplet manipulation system. Fig. 3(a) and 3(b) show infrared images of two complementary checkerboard thermal maps taken by thermography equipment (TVS-500EX, NEC Avio Infrared Tech. Co.), displaying the largest temperature contrast of the adjacent TE chips. The highest and lowest reachable temperatures of the 2D array are ~83 °C and ~17 °C, respectively. The achievable temperatures of the TE chips in the 2D array are slightly increased because the tightly-packed arrangement of the 2D array allows heat exchange between neighboring TE chips, resulting in a challenging condition for the air-cooling heatsink/fan system below the chips. Fig. 3(c) and 3(d) show infrared images of two complementary checkerboard thermal maps for the 2D array with an overlaid 0.7 mm thick glass attached by a

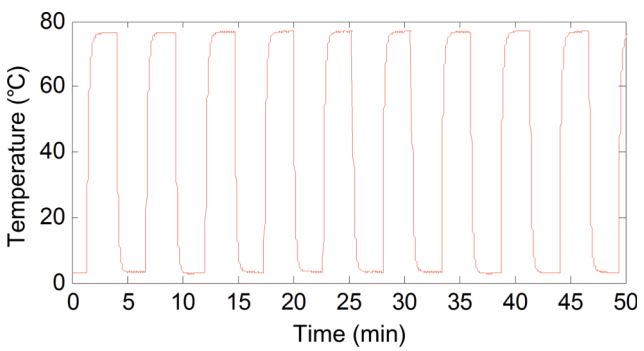

Fig. 2 Thermal cycle test with the maximum reachable temperature range for a single TE chip.

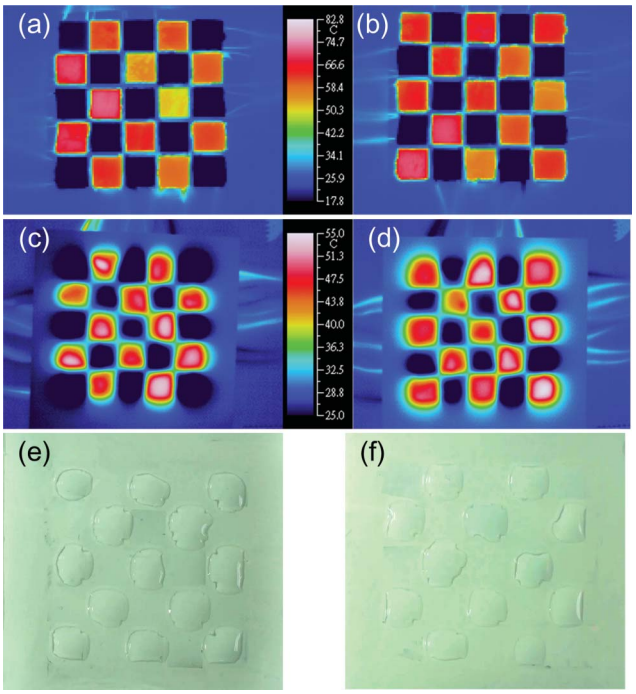

Fig. 3 Thermographs of the generated thermal maps for (a)(b) bare TE array; (c)(d) TE array with an overlying hydrophobically patterned glass substrate; (e)(f) the confined liquid morphology corresponding to (c)(d).

thermal conducting paste. Similarly, because of the lateral thermal conduction through the glass substrate, the temperature contrast between neighboring TE chips reduces and the reachable temperature range falls within 55 °C and 25 °C. Fig. 3(e) and 3(f) are the liquid morphologies corresponding to the thermal maps of Fig. 3(c) and 3(d), respectively. Though the achievable temperature range is reduced, it clearly demonstrates that this checkerboard thermal map can successfully draw and confine the deposited liquid into the colder regions. The liquid morphology can be successfully switched between these two thermal map configurations.

Fig. 4 plots sequential snapshots for liquid routing, merging, and splitting on the patterned glass substrate. Initially, two dodecane liquid droplets are located on the upper two corners of the patterned substrate, as shown in Fig. 4(a). Next, as shown in Fig. 4(b) and 4(c), these two droplets are manipulated toward each other by the following control strategy: (i) heating up beneath the TE chip, where the droplet is pushed away from its current position; (ii) cooling the adjacent TE chip which locates the motion direction of the droplet; and (iii) heating up the remaining adjacent TE chips, to avoid the unwanted advances of the droplet onto these chips. Then, the droplets are programmed to merge, where Fig. 4(d) and 4(e) show the snapshots at and after the merge, respectively. The merged droplet is then driven downwards as shown in Fig. 4(f)–4(i). Similarly, the TE chips on the left, right, above, and beneath the droplet in these snap shots are heated. Following that, the merged droplet is manipulated to separate by heating up TE chip underneath and cooling the left and right adjacent TE chips; Fig. 4(j) and 4(k) show the moments at and after the successful separation, accordingly. Finally, the droplets are driven into the lower two corners as shown in Fig. 4(l).

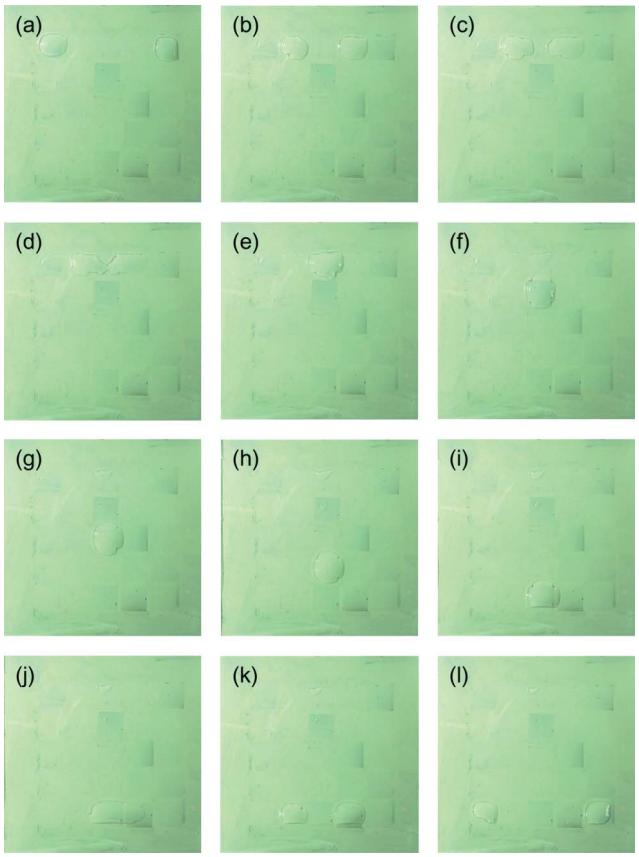

Fig. 4 Snapshots of droplet actuation, merging, and splitting on the hydrophobically patterned glass substrate.

4. Summary

We successfully implement a 5 × 5 TE array for a 2D free-surface thermocapillary droplet actuation. The advantage of using TE chips over the traditional resistance heaters is the bi-directional temperature controllability. With the presented 2D setup, the achievable temperature range of the adjacent TE chips falls between ~53 °C and ~25 °C with an overlaid 0.7 mm glass substrate on the TE array. The liquid droplets can be successfully routed, merged, and split using the programmed thermal maps.

Acknowledgements

M.C.L., J.G.W., and M.F.T. are supported by Undergraduate Grant Project NSC 99-2815-C-002-082-E from National Science Council of Taiwan. J.Z.C. gratefully acknowledges the funding support from the National Science Council of Taiwan under the grant nos. NSC 100-2627-M-002-002, NSC 97-2221-E-002-052, and NSC 97-2218-E-002-024. The authors also like to express gratitude toward Prof. Wen-Pin Shih, in Department of Mechanical Engineering at National Taiwan University, for the access to the thermography equipment. The kind support for the equipment and technical consulting from the National Instruments Taiwan Branch are also gratefully acknowledged.

References

1 M. A. Burns and T. S. Sammarco, *AIChE J.*, 1999, **45**, 350–366.
2 M. A. Burns and N. Srivastava, *Lab Chip*, 2006, **6**, 744–751.
3 M. C. Wu, A. T. Ohta, A. Jamshidi, J. K. Valley and H. Y. Hsu, *Appl. Phys. Lett.*, 2007, **91**, 074103.
4 Z. J. Jiao, N. T. Nguyen and X. Y. Huang, *J. Micromech. Microeng.*, 2007, **17**, 1843–1852.
5 N. T. Nguyen, Z. J. Jiao and X. Y. Huang, *Sens. Actuators, A*, 2007, **140**, 145–155.
6 N. T. Nguyen, Z. J. Jiao, X. Y. Huang and Y. Z. Ang, *Microfluid. Nanofluid.*, 2007, **3**, 39–46.
7 X. Y. Huang, Z. J. Jiao, N. T. Nguyen and P. Abgrall, *Microfluid. Nanofluid.*, 2008, **5**, 205–214.
8 M. L. Cordero, D. R. Burnham, C. N. Baroud and D. McGloin, *Appl. Phys. Lett.*, 2008, **93**, 034107.
9 N. T. Nguyen, Y. F. Yap, S. H. Tan, S. M. S. Murshed, T. N. Wong and L. Yobas, *J. Phys. D: Appl. Phys.*, 2009, 42.
10 J. B. Brzoska, F. Brochard-Wyart and F. Rondelez, *Langmuir*, 1993, **9**, 2220–2224.
11 M. L. Ford and A. Nadim, *Phys. Fluids*, 1994, **6**, 3183–3185.
12 M. K. Smith, *J. Fluid Mech.*, 1995, **294**, 209–230.
13 A. A. Darhuber, J. P. Valentino, S. M. Troian and S. Wagner, *J. Microelectromech. Syst.*, 2003, **12**, 873–879.
14 J. Z. Chen, A. A. Darhuber, S. M. Troian and S. Wagner, *Lab Chip*, 2004, **4**, 473–480.
15 C. C. Cheng, Y. T. Tseng, F. G. Tseng and Y. F. Chen, *Sens. Actuators, A*, 2004, **114**, 292–301.
16 J. Z. Chen, S. M. Troian, A. A. Darhuber and S. Wagner, *J. Appl. Phys.*, 2005, **97**, 014906.
17 R. S. Subramanian, V. Pratap and N. Moumen, *Langmuir*, 2008, **24**, 5185–5193.
18 A. A. Darhuber, J. P. Valentino and S. M. Troian, *Lab Chip*, 2010, **10**, 1061–1071.
19 H. B. Nguyen and J. C. Chen, *Phys. Fluids*, 2010, **22**, 062102.
20 W. Hu and A. T. Ohta, *Microfluid. Nanofluid.*, 2011, **11**, 307–316.
21 J. P. Valentino, S. M. Troian and S. Wagner, *Appl. Phys. Lett.*, 2005, **86**, 184101.
22 Y. Zhao, F. Liu and C.-H. Chen, *Appl. Phys. Lett.*, 2011, **99**, 104101.
23 M. Akbari, M. Bahrami and D. Sinton, *Microfluid. Nanofluid.*, 2011, DOI: 10.1007/s10404-011-0866-6.